

Ferromagnetism in Co doped CeO₂: Observation of a giant magnetic moment with a high Curie temperature

Ashutosh Tiwari^{a)}

NanoStructured Materials Research Laboratory (NMRL), Department of Materials Science & Engineering, University of Utah, Salt Lake City, Utah 84112

V. M. Bhosle, S. Ramachandran, N. Sudhakar, and J. Narayan

Department of Materials Science & Engineering, North Carolina State University, Raleigh, North Carolina 27695-7916

S. Budak and A. Gupta

Center for Materials for Information Technology, University of Alabama, Tuscaloosa, Alabama 35487

(Received 16 November 2005; accepted 25 February 2006; published online 7 April 2006)

We report room temperature ferromagnetism in single crystal Ce_{1-x}Co_xO_{2-δ} ($x \leq 0.05$) films deposited on a LaAlO₃(001) substrate. Films were grown by a pulsed laser deposition technique and were thoroughly characterized using x-ray diffraction, high-resolution transmission electron microscopy coupled with electron energy loss spectroscopy and scanning transmission electron microscopy-Z contrast, x-ray photoelectron spectroscopy, optical transmission spectroscopy, and magnetic measurements. These films are transparent in the visible regime and exhibit a very high Curie temperature ~ 740 – 875 K with a giant magnetic moment. Our results indicate that the ferromagnetic property is intrinsic to the CeO₂ system and is not a result of any secondary magnetic phase or cluster formation. © 2006 American Institute of Physics. [DOI: [10.1063/1.2193431](https://doi.org/10.1063/1.2193431)]

Spintronics is a fast emerging field that utilizes both charge as well as the spin degrees of freedom of electrons. It has the potential to enormously enhance data processing and the storage capacity of present-day devices. The most critical step in the functioning of a spintronic device is the injection and detection of spin-polarized carriers at the ferromagnet-semiconductor interface. Despite considerable efforts, the efficient injection of spins into nonmagnetic semiconductors still continues to be a challenging problem. In order to solve this problem, it is desirable to have ferromagnetic semiconductors, which can integrate the spin functionality of electrons with semiconducting characteristics of the material.

The quest for the search of ferromagnetic semiconductors is not new; the very first report about the observation of ferromagnetism in semiconductors came as early as 1961 when Matthias *et al.*¹ reported ferromagnetism in europium chalcogenides EuX (X: O, S, Se) with $T_c \sim 69$ K. Later on, low temperature (< 300 K) ferromagnetism was observed in several other compound semiconductor materials^{2–4} when doped with a small amount of transition metal elements. Recently, extensive research has been performed on diluted magnetic semiconductor (DMS) systems, with the major focus on creating room temperature ferromagnetic (RTF) semiconductors. A major boost to these efforts was realized by a theoretical work by Dietl *et al.*⁵ in which they predicted the RTF in Mn doped ZnO and GaN. Just within a few years of this work, RTF has been observed in several DMS systems^{6–9} containing a small amount of transition metal elements doped in semiconducting matrices.

Most of the room temperature ferromagnetic DMS materials discovered so far have noncubic crystal symmetry. However, it is anticipated that if one can introduce room temperature ferromagnetism in cubic systems, then it will facilitate the integration of spintronic devices with advanced silicon based microelectronic devices. In this letter, we report

the observation of RTF in a face centered cubic system having a fluorite crystal structure. The system consists of a matrix of cerium oxide (CeO₂) doped with a small amount of cobalt. Cerium oxide is a transparent rare-earth oxide possessing a high dielectric constant ($\epsilon = 26$) that is closely lattice matched with silicon.

Ce_{1-x}Co_xO_{2-δ} films were grown on LaAlO₃ (001) substrates by a pulsed laser ablation of highly dense pellets. Films were characterized using x-ray diffraction, high-resolution transmission electron microscopy (HRTEM), x-ray photoelectron spectroscopy (XPS), and optical absorption spectroscopy at room temperature. Magnetic property measurements were performed using two different techniques: in the temperature range 5–300 K a superconducting quantum interference device (SQUID) magnetometer was used, while in the temperature range 300–900 K, we employed a vibrating sample magnetometer (VSM).

An x-ray diffraction pattern of the Ce_{1-x}Co_xO_{2-δ} films showed diffraction peaks corresponding to a (001) family of planes only indicating a strong *c* axis alignment of the film. A high-resolution cross-sectional TEM image from a Ce_{0.97}Co_{0.03}O_{2-δ}/LaAlO₃ interface is shown in Fig. 1(a), the inset shows the fast Fourier transform (FFT) pattern from a part of the film. Selected area electron diffraction (SAED) patterns from the Ce_{0.97}Co_{0.03}O_{2-δ}/LaAlO₃ interface are shown in Fig. 1(b). Well-aligned spots demonstrate very good crystal quality and a phase purity of the Ce_{0.97}Co_{0.03}O_{2-δ} films. Indexing of these patterns gives the following orientational relationship between the film and substrate: $[001]_{\text{CeO}_2} \parallel [001]_{\text{LaAlO}_3}$ and $[220]_{\text{CeO}_2} \parallel [020]_{\text{LaAlO}_3}$. This implies that the *c* axis (out of plane) of CeO₂ is parallel to the *c* axis of LaAlO₃ with a 45° in-plane rotation between the film and the substrate, where the {220} planes of the film are aligned with the {200} planes of the substrate via domain matching epitaxy.¹⁰ Our x-ray photoelectron spectroscopy (XPS) results showed that in these films cobalt ions are

^{a)}Electronic mail: tiwari@eng.utah.edu

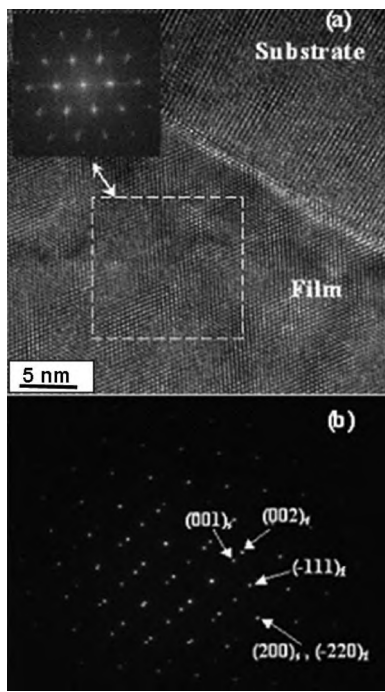


FIG. 1. (a) HRTEM image from a $\text{Ce}_{0.97}\text{Co}_{0.03}\text{O}_{2-\delta}/\text{LaAlO}_3$ interface. The inset shows FFT from a region marked in the figure. (b) Cross-sectional SAED pattern from $\text{Ce}_{0.97}\text{Co}_{0.03}\text{O}_{2-\delta}/\text{LaAlO}_3$ combined.

present in the mixed valence state, with Co^{2+} and Co^{3+} existing together.

Figure 2 shows the optical transmittance data for a $\text{Ce}_{0.97}\text{Co}_{0.03}\text{O}_{2-\delta}$ film. For comparison, we have also shown the corresponding data for undoped CeO_2 . As can be seen in this figure, the absorption edge for $\text{Ce}_{0.97}\text{Co}_{0.03}\text{O}_{2-\delta}$ is located at a slightly lower wavelength compared to undoped CeO_2 . This shift in the absorption edge again confirms the matrix incorporation of cobalt in the system. In the inset, we have shown an optical image demonstrating the high transparency of the $\text{Ce}_{0.97}\text{Co}_{0.03}\text{O}_{2-\delta}$ film in the visible range of the spectrum. A sharp absorption peak at 360 nm corresponds to an optical gap of 3.4 eV and can be associated with the electronic band structure of CeO_2 .^{11,12} In the band-gap regime the optical spectrum is strongly affected by interference effects and clearly distinguishable interference fringes can be envisaged. Above the wavelength of 700 nm, a dip in the transmission data is observed, which suggests the presence of a significant amount of midgap defect states in the system. Earlier studies about defect states in CeO_2 have

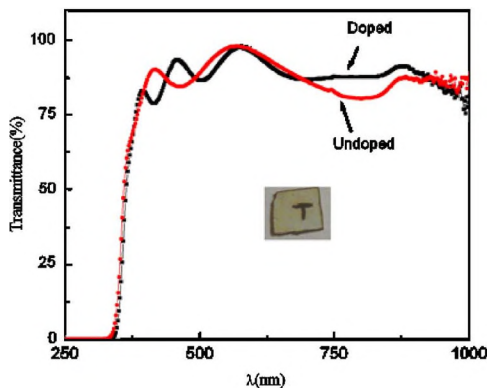


FIG. 2. Optical transmission spectra from the $\text{Ce}_{0.97}\text{Co}_{0.03}\text{O}_{2-\delta}$ and CeO_2 films. The inset shows an optical image demonstrating the high transparency of the $\text{Ce}_{0.97}\text{Co}_{0.03}\text{O}_{2-\delta}$ film in the visible range of the spectrum.

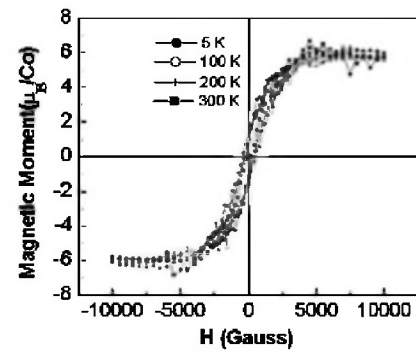


FIG. 3. Magnetization loop (M vs H) for $\text{Ce}_{0.97}\text{Co}_{0.03}\text{O}_{2-\delta}$ at different temperatures.

also shown that it is quite prone to oxygen vacancies, while it still retains its fluorite crystal structure over a wide range of nonstoichiometric compositions through the inclusion of oxygen vacancies.^{11–13}

In Fig. 3, we have shown typical magnetization versus field curves of $\text{Ce}_{0.97}\text{Co}_{0.03}\text{O}_{2-\delta}$ at different temperatures. As evident from this figure, $\text{Ce}_{0.97}\text{Co}_{0.03}\text{O}_{2-\delta}$ exhibits room temperature ferromagnetism. Figure 4 shows the magnetization of a $\text{Ce}_{0.97}\text{Co}_{0.03}\text{O}_{2-\delta}$ film as a function of temperature. Magnetization at 5 K is $6.1 \pm 0.2 \mu_B/\text{Co}$ atom and remains quite constant up to about 500 K. Above 500 K it starts increasing and attains a maximum value of $8.2 \pm 0.2 \mu_B/\text{Co}$ atom at around 725 K. Beyond this temperature the magnetization drops monotonically showing a Curie temperature at about 875 K. An occurrence of such a high transition temperature with a giant magnetic moment in transparent $\text{Ce}_{1-x}\text{Co}_x\text{O}_{2-\delta}$ films is remarkable. This is the highest moment of cobalt ever observed in any oxide system and is even higher than that reported recently by Ogale *et al.*⁹ in Co doped SnO_2 films. The inset of Fig. 4 shows the magnetization of a $\text{Ce}_{0.95}\text{Co}_{0.05}\text{O}_{2-\delta}$ film as a function of temperature. It is clear from the figure that the net magnetic moment of a $\text{Ce}_{0.95}\text{Co}_{0.05}\text{O}_{2-\delta}$ film is slightly less than that of a $\text{Ce}_{0.97}\text{Co}_{0.03}\text{O}_{2-\delta}$ film and it exhibits a rather different temperature dependence. The dashed line represents the extrapolated curve obtained by fitting low temperature data to the standard M vs T relation for a ferromagnet. From this analysis, we obtained a transition temperature of 725 K. Since we did not observe any kind of nanoclusters in the HRTEM, we infer that the presence of nanoclusters could not be the cause of the observed high-temperature ferromagnetism. Further-

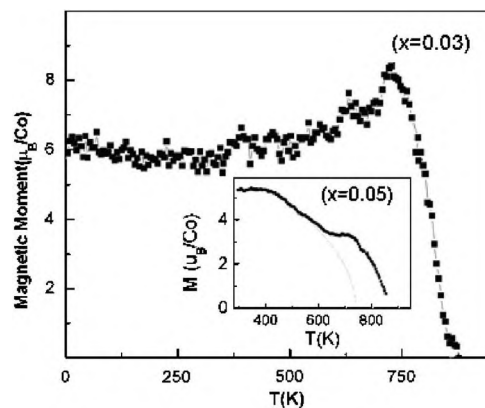


FIG. 4. Saturation magnetization as a function of temperature for $\text{Ce}_{0.97}\text{Co}_{0.03}\text{O}_{2-\delta}$. The inset shows the magnetization of the $\text{Ce}_{0.95}\text{Co}_{0.05}\text{O}_{2-\delta}$ film as a function of temperature.

more, if nanoclusters were of such a small size that they could not be detected by the HRTEM, then they should exhibit superparamagnetic behavior with a much lower blocking temperature, which was not the case.

A cobalt ion (Co^{2+} as well as Co^{3+}) can exist in two different spin configurations, namely, the high spin state and the low spin state. If it is in the low spin state, then the maximum spontaneous moment (assuming it is in the Co^{2+} state) it can have is $M \sim 1.7\mu_B$ [$M = g\mu_B\sqrt{S(S+1)}$; $g=2$, $S=1/2$].¹⁴ On the other hand, if Co ions are in high spin states, S can have the maximum value of 2 (assuming all Co ions to be in the Co^{3+} state), which will result in the spontaneous moment of $\sim 4.9\mu_B$. These moments are much smaller than the observed values. Now, if we consider the possibility that in our films orbital moments of Co are unquenched, then the maximum net angular momentum of Co will be $J=L+S=4$ and it will possess a spontaneous magnetic moment of $M \sim 6.7\mu_B$ [$M = g\mu_B\sqrt{J(J+1)}$; $g=3/2$, $J=4$].¹⁴ This value is very close to the magnetic moment observed at low temperatures, however, the maximum magnetic moment of the system (at 740 K) is still higher by about 22%. This implies that the observed magnetic moment at higher temperatures not only is from Co ions, but also has a significant contribution from the surrounding CeO_2 , which has been magnetically polarized. If we assume that Co is in a high spin state with an unquenched orbital angular momentum and we attribute an extra magnetic moment to Ce then each formula unit of CeO_2 will have a net moment of $0.05\mu_B$.

The observation of unquenched orbital moments of cobalt in an insulating oxide matrix is quite rare though this phenomenon has quite often been observed in cobalt doped in alkali metals.¹⁵ As a matter of fact, in the isolated state, atoms of almost all the transition metal elements possess large orbital as well as spin magnetic moments. But in the solid state, because of hybridization and crystal field splitting, these moments get reduced. Diluted magnetic systems lie in between these two extremes. In these materials (provided individual transition metal atoms are far apart) the magnetic moment can still remain unquenched. However, in these systems even a slight increase in the dopant concentration is likely to result in the progressive quenching of the orbital moments due to the enhanced interaction among the dopant atoms. The decrease in the magnetic moment for our higher Co doped film fits very well with the above picture supporting the presence of unquenched orbital moments.

In insulating materials, magnetic ordering is usually caused by superexchange coupling, but the coupling results in antiferromagnetic ordering. Another plausible mechanism, which has recently been proposed to explain the ferromagnetism in some transparent oxides is an F -center mediated exchange mechanism. An F center consists of an electron trapped in an oxygen vacancy. Electrons in an F center remain effectively bound to a positively charged center and possess a spectrum of energy levels. Since earlier electron spin resonance experiments have shown the abundance of F centers in CeO_2 (as a result of the trapping of electrons in oxygen vacancies),¹⁶ we believe this mechanism also plays an important role in the $\text{Ce}_{1-x}\text{Co}_x\text{O}_2$ films. For F centers, the radius of the electron orbital is given by $\sim a_0\epsilon$, where a_0 is the Bohr radius and ϵ is the dielectric constant of the material. In CeO_2 ($\epsilon=26$) the radius of the F electron orbital is

estimated to be $\sim 14 \text{ \AA}$, which is sufficiently large to mediate ferromagnetic coupling among Co ions.

Another aspect that needs to be further addressed is the magnetic polarization of the CeO_2 matrix. The mechanism responsible for this behavior is not very clear at this moment. However, we speculate that it could be arising because of the transfer of some electrons from the impurity bands to the empty $4f$ bands of Ce^{4+} at higher temperatures. This speculation is supported by the unusual shape of M vs T curves, where an increase in the value of magnetization is observed at a higher temperature. Further spectroscopic investigations are needed to understand this aspect fully. At this point we find it relevant to mention that a similar kind of magnetic polarization has recently been reported¹⁷ in another highly insulating dielectric system (HfO_2).

In conclusion, we have observed high temperature ferromagnetism in $\text{Ce}_{1-x}\text{Co}_x\text{O}_{2-\delta}$ films grown by a pulsed laser deposition technique on the $\text{LaAlO}_3(001)$ substrate. These films are transparent and exhibit a giant magnetic moment. Our results show that in these films not only the orbital magnetic moment of cobalt remains unquenched but also the CeO_2 matrix gets magnetically polarized. We believe that the observation of high temperature ferromagnetism with such a high magnetic moment and transition temperature in a lightly doped high- k dielectric material represents a groundbreaking step in the field of spintronics.

One of the authors (A.T.) thanks all the members of the Nanostructured Materials Research Laboratory of the University of Utah for excellent support. Research at the University of Alabama was supported by an NSF-MRSEC grant.

¹B. T. Matthias, R. M. Bozorth, and J. H. Van Vleck, *Phys. Rev. Lett.* **7**, 160 (1961).

²H. Ohno, A. Shen, F. Matsukura, A. Oiwa, A. Endo, S. Katsumoto, and Y. Iye, *Appl. Phys. Lett.* **69**, 363 (1996); H. Ohno, *Science* **281**, 951 (1998).

³T. Fukumura, Z. W. Jin, A. Ohtomo, H. Koinuma, and M. Kawasaki, *Appl. Phys. Lett.* **75**, 3366 (2000).

⁴G. A. Prinz, *Science* **282**, 1660 (1998).

⁵T. Dietl, H. Ohno, F. Matsukura, J. Cibert, and D. Ferrand, *Science* **287**, 1019 (2000).

⁶S. Ramachandran, A. Tiwari, and J. Narayan, *Appl. Phys. Lett.* **84**, 5255 (2004); A. Tiwari, C. Jin, A. Kvit, D. Kumar, J. F. Muth, and J. Narayan, *Solid State Commun.* **121**, 371 (2002); P. Sharma, A. Gupta, K. V. Rao, F. J. Owens, R. Sharma, R. Ahuja, J. M. O. Guillen, B. Johansson, and G. A. Gehring, *Nat. Mater.* **2**, 673 (2003).

⁷Y. Matsumoto, M. Murakami, T. Shono, T. Hasegawa, T. Fukumura, M. Kawasaki, P. Ahmet, T. Chikyow, S.-Y. Koshihara, and H. Koinuma, *Science* **291**, 854 (2001).

⁸S. A. Chambers, S. Thevuthasan, R. F. C. Farrow, R. F. Marks, J. U. Thiele, L. Folks, M. G. Samant, A. J. Kellock, N. Ruzycski, D. L. Ederer, and U. Diebold, *Appl. Phys. Lett.* **79**, 3467 (2001).

⁹S. B. Ogale, R. J. Choudhary, J. P. Buban, S. E. Lofland, S. R. Shinde, S. N. Kale, V. N. Kulkarni, J. Higgins, C. Lanci, J. R. Simpson, N. D. Browning, S. Das Sarma, H. D. Drew, R. L. Greene, and T. Venkatesan, *Phys. Rev. Lett.* **91**, 077205 (2003).

¹⁰J. Narayan and B. C. Larson, *J. Appl. Phys.* **93**, 278 (2003).

¹¹T. Inoue, Y. Yamamoto, and M. Satoh, *Thin Solid Films* **343**, 594 (1999).

¹²A. H. Morshed, M. E. Moussa, S. M. Bedair, R. Leonard, S. X. Liu, and N. El-Masry, *Appl. Phys. Lett.* **70**, 1647 (1997).

¹³H. L. Tuller and A. Nowick, *J. Phys. Chem. Solids* **38**, 859 (1977).

¹⁴N. W. Ashcroft and N. D. Mermin, *Solid State Physics* (Harcourt College Publishers, Fort Worth, TX, 1975).

¹⁵H. Beckmann and G. Bergmann, *Phys. Rev. Lett.* **83**, 2417 (1999); G. Bergmann and M. Hossain, *Phys. Rev. Lett.* **86**, 2138 (2001); P. Gambardella, S. S. Dhesi, S. Gardonio, C. Grazioli, P. Ohresser, and C. Carbone, *Phys. Rev. Lett.* **88**, 047202 (2002).

¹⁶I. Vinokurov, Z. Zom, and V. Ioffe, *Sov. Phys. Solid State* **9**, 2659 (1968).

¹⁷M. Venkatesan, C. B. Fitzgerald, and J. M. D. Coey, *Nature (London)* **430**, 630 (2004).